Engenharia Agrícola

ISSN: 1809-4430 (on-line)

www.engenhariaagricola.org.br

Scientific Paper
Doi: http://dx.doi.org/10.1590/1809-4430-Eng.Agric.v42n4e20210066/2022

DESIGN AND EXPERIMENT OF KEY COMPONENTS OF PADDY FIELD WEEDING DEVICE

Liang Tian[1] , Jun Ge[1,2] , Liangfei Fang[1] , Kuan Qin[1*,2] , Chengmao Cao [1*,2]

[1*] Corresponding author. Anhui Agricultural University/ Hefei, China.
E-mail: qinkuan@ahau.edu.cn | ORCID ID: https://orcid.org/ 0000-0002-4411-9631
E-mail: caochengmao@sina.com | ORCID ID: https://orcid.org/ 0000-0002-0505-4994

KEYWORDS

agricultural machinery, weed control, intra-row weeding, discrete element method simulation.

ABSTRACT

A type of weeding device was designed to solve the problems of weeders in paddy fields, such as high rice seedling damage and low weeding rate. The structure of the weeding machine and the working principle are illustrated. The seedling avoiding and weeding mechanism of the weeding device were analyzed. The parts of the weeder that contacted the soil were designed. The contact process between the spring tine and soil in paddy was simulated using the discrete element method to study the change in mechanical behavior during the working process. To verify the performance of the weeding machine, the forward speed and hoeing depth were taken as experimental factors, and weeding rate and rice seedling damage rate were selected as test indices. Field experiments were conducted to study the effects of each factor on weeding operations. The results of the experiment were evaluated by multi-index comprehensive weighting. The test results showed that, when the forward speed was 0.30 m/s and hoeing depth was 40 mm, rice seedling damage rate was 3.4%, weeding rate was 85%. The weeding machine satisfies the requirements of weeding in paddy. This research can provide a reference for the design of intra-row weeding devices in paddy.

INTRODUCTION

Organic agriculture requires the use of herbicides and pesticides to be minimized or even eliminated (Boone et al., 2019; Jia et al., 2018). Mechanical weeding is an environmentally friendly method of weeding without chemical pollution (Qi et al., 2015; Qi et al., 2017). During the process of weeding, mechanical weeding components can plow the soil, increase the oxygen content of the soil, and promote the absorption of nutrients by crops (Qi et al., 2016; Pannacci et al., 2020; Zhang & Chen, 2017; Alba et al., 2020). Therefore, mechanical weeding has become a trend in the development of green agriculture. Improving the rate of weeding and reducing the rate of damage to seedlings has always been core topics in mechanical weeding research. At present, inter-row mechanical weeding technology has been widely used, but there are not many studies on intra-row mechanical weeding technology (Hu et al., 2013). Compared with inter-row weeds, intra-row weeds are closer to crops and divide the intra-row space into discontinuous areas. Therefore, intra-row mechanical weeding operations are difficult to perform and require high precision (Pérez-Ruíz et al. 2014; Hu et al. 2012), and thus damage to the rice seedlings can more easily occur than the inter-row weeding.

To control intra-row weeds, domestic and foreign researchers have undertaken a series of studies on intra-row weeding machines. Halmstad University has developed an intra-row weed control system (Åstrand et al., 2002; Persson & Åstrand, 2008). The weeding device used a rotating weeding wheel perpendicular to the crop rows to prevent and control intra-row weeds. The crops were identified through computer vision. When crops were detected, the rotating wheel was driven upward by a pneumatic cylinder to avoid damage to the crops. After the rotating wheel avoided the crops, it was repositioned to continue the weeding operation. The cultivating system developed by Home (Home, 2003) consists of a "duck-foot" type inter-row weeding knife and an intra-row weeding knife. When crops were detected, the intra-row weeding knife was closed; otherwise, the motor drove the cam to unfold the intra-row weeding knife. The weeding

[1] School of Engineering, Anhui Agricultural University/ Hefei, China.
[2] Scientific observing and experimental Station of Agricultural Equipment for the Southern China. Ministry of Agriculture and Rural Affairs of the People's Republic of China/ Hefei, China.

Area Editor: João Paulo Arantes Rodrigues da Cunha
Received in: 4-24-2021
Accepted in: 7-2-2022

part of the rotary disk hoe developed by Tillett (Tillett et al., 2007) was a rotatable disk. To control weeds between plants without damaging crops, a part of the edge of the rotary disk was cut off to form a gap. The weeds were distinguished from the crops using machine vision. When the weeding machine was pulled forward by the tractor, the rotating disk rotated to ensure that the gap was always aligned with the crops.

The weeding machine in paddy fields developed by Wang Jinwu (Wang et al., 2018; Tao et al., 2015) used a steel-wire flexible shaft to drive the spring tooth disk to rotate. The spring tine stirred and turned the soil, uprooted the weeds, and buried the intra-row weeds to remove them from their roots. The planetary brush-type intra-row manipulator weeding device developed by Chen Ziwen (Chen et al., 2015a; Chen et al., 2015b; Li et al., 2016) used an eccentric knife bar to make the manipulator rotate away from the crop rows or within the crop rows. The cam-rocker-type intra-row weeding device studied by Zhou Fujun (Zhou et al., 2018) converted the rotation of the motor into the reciprocating swing of the weeding knife by a cam rocker mechanism. The size of crop protection areas was adjusted by replacing the cams to suit the different weeding fields.

Intelligent weeding device, because of its installation of intelligent device, has long reaction time, low efficiency, high price, poor adaptability and other problems. Mechanical weeding has some problems, such as low weeding rate, high damage rate and poor adaptability.

To solve the problems of high rice seedling damage rate and low weeding rate in the existing weeding machines in paddy fields, a swing-type intra-row weeding device was designed. The working principle of the weeding machine was described. The key components of the weeding device were designed using a parameterization method. To study the change in mechanical behavior of the soil-contact parts, the contact processes between the spring tine and the soil in the paddy were simulated by using the discrete element method. Field experiments were conducted to test the working performances of the weeding machine. So as to provide a reference for designing intra-row weeding machines in paddy fields.

MATERIAL AND METHODS

Overall structure and working principle

The structure of the weeding device prototype developed in this study is shown in Figure1. It is mainly composed of frames, walking devices, inter-row weeding devices, intra-row weeding devices, suspension devices, anti-winding knives, depth limit plates, mud scrapers, and hoeing depth adjustment devices. A gasoline engine provides power for the weeding device of the prototype, driving the weeding wheels to rotate and the spring tines to swing. The weeding device is located between the front and rear walking wheels, in front of the driver's seat, so that the driver can observe the weeding operation.

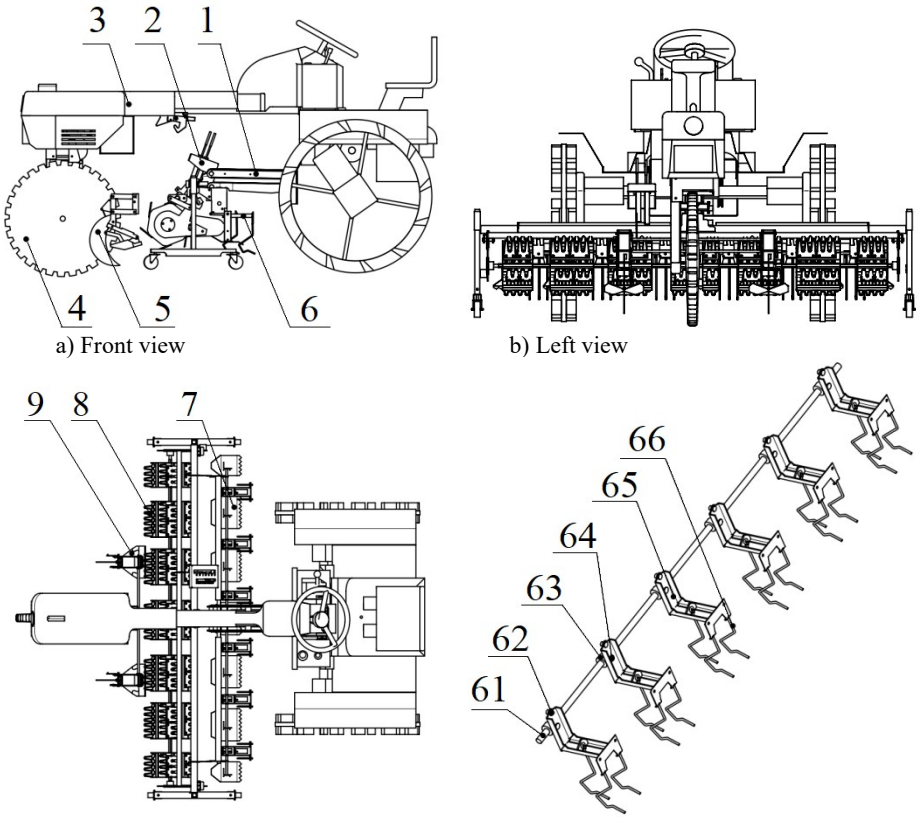

a) Front view b) Left view

c) Top view d) Structural diagram of intra-row weeding device

1. Suspension device. 2. Hoeing depth adjusting device. 3. Frame. 4. Walking device. 5. Anti-winding knife. 6. Intra-row weeding device. 61. Intra-row drive shaft. 62. Rocking shaft. 63. Rotating the sleeve. 64. Oscillating rod. 65. Spring tine rack. 66. Spring tine. 7. Mud scraper. 8. Inter-row weeding device. 9. Depth limit plate.

FIGURE 1. Overall structural schematic of the weeding machine.

In the field operation, the hoeing depth is adjusted according to the seedling and weed growth of the working field, so that the weeding device can meet the operational requirements of different fields. As the weeding device advances, the inter-row weeds in the paddy fields are removed by the rotating weeding wheels, and the intra-row weeds in the paddy fields are removed by the spring tines that swing from side to side. During the rotation of the weeding wheel, the rake teeth enter the soil to remove inter-row weeds. After weeding, the rake teeth are raised off the ground, and the soil is thrown backward. The machine uses this method to loosen the soil and kill weeds. The spring tine moves forward along the crop seedling belt and swings at the same time. The intra-row weeds in paddy fields were pulled out or pressed into the soil. The weeds pulled out are unable to absorb nutrients and gradually wither; the weeds pressed into the soil are buried by paddy mud, unable to undergo photosynthesis, and die.

Weeding principle

The weeds in paddy fields are mainly gramineous weeds such as barnyard grass and *Leptochloa chinensis*, accompanied by a small amount of Cyperaceae weeds and broad-leaved weeds (Zhou et al., 2019). Barnyard grass belongs to the Gramineae family of weeds and is strongly associated with rice. It is one of the most harmful weeds in paddy fields, seriously affecting the yield and quality of rice (Zhang & Gong, 2014; Agriculture-Field Crops, 2020). In this study, we take barnyard grass as an example to illustrate the weeding principle of the weeding device. The weeds mentioned later refer to barnyard grass.

Rice, a major staple in China, is an annual gramineous plant (Zhu et al., 2015; Zheng et al., 2020; Zhang et al., 2014). The growth characteristics of barnyard grass are very similar to those of rice, and they both experience seedling, tillering, and heading stages. The germination time of weeds and rice is inconsistent, but there is a certain time difference in the growth and development periods. Although barnyard grass is strongly associated with rice, it does not grow synchronously. Based on the asynchronous growth cycle of rice and weeds, this article analyzes the similarities and differences between the root growth of seedlings and weeds and explains the weeding principle of the weeding device.

The root systems of barnyard grass and rice are very similar; both are fibrous root systems, including the main and secondary roots (Yang et al., 2016; Xu et al., 2015). Weeds in paddy fields begin to germinate 3–5 days after planting seedlings, and a peak of grass emerges on the 7th day (Zhou et al. 2020). Rice seedlings end the greening stage and enter the tillering stage about seven days after transplanting. The roots of rice are composed of a main radicle and secondary radicles with a flat oval distribution of roots. During this period, the paddy field weeds are in the germination stage, and a few weeds enter the seedling stage, with only one weak main root, and the secondary roots have not yet grown or only a few roots have grown.

Therefore, the root system of rice and the root system of weeds are quite different in this period. Rice is stronger than weeds, and it is relatively simple to remove weeds. When the weeds enter the tillering stage, the secondary roots of the weeds grow in large numbers and form a developed root system. The difference between the weeds and the rice roots gradually decreases, even surpassing that of rice. At this time, weeding becomes difficult. There is a competitive relationship between weeds and rice (Tian et al., 2020). They compete for sunlight and nutrients. The more vigorous weeds grow and the more field nutrients they consume, the less nutrients the rice can absorb. Therefore, the stronger the weeds grow, the more difficult it is to weed, and the higher the cost of weeding.

According to the above analysis, it can be seen that the best period for weeding in paddy fields is about a week after transplanting. At this time, weeds have just begun to grow and develop, which is quite different from the seedlings, and they have little effect on the growth of seedlings. Weeding is easier during this time. The weeds that germinate after the second weeding operation are much weaker than the rice seedlings, and they cannot form a competitive relationship with rice seedlings. Investigation (Wang et al., 2017; Niu & Wang, 2010) reveals that, about a week after transplanting, the root depth of rice seedlings is 8–10 cm, the root area diameter does not exceed 3 cm, and the root depth of weeds is only 3–5 cm.

When the weeding device operates in the paddy field, the spring tine touches the rice seedlings or weeds, generating a F_f. This force continues to act on the paddy field plants. When the force F_f is greater than the soil resistance to plant roots, the plant moves with the spring tine, leaving the original position in the soil. The plant is then pressed into or pulled out of the soil. During weeding, the main root of the rice seedling moves with the spring tine. When the main root reaches a certain position, the secondary roots of the seedling pull the main root. The lower end of the main root bends upward to avoid the thrust of the spring tine. Then, the spring tine moves away from the soil, and the rice seedling keeps it intact. The secondary roots of rice seedlings are a thick elliptical root system. If the secondary roots of rice seedlings contact the spring tine, they will be affected by the resistance of the soil and the pushing force of the spring tine. The rice seedling leaves the soil with the spring tine, which damages the seedling. When the rice seedling is subjected to the force F_f from the spring tine, the change in the root is shown in Figure 2. Rice is a type of plant with a fibrous root system, so its subsequent growth will not be affected when its root is slightly damaged.

During the weeding operation, the barnyard grass is in the germination period and has not entered the tillering period, and the secondary roots have not yet formed. Hence, only the main root is affected by the soil resistance and the spring tine thrust. It is pulled out or pressed into the soil with the swing of the spring tine. This completes the weeding operation.

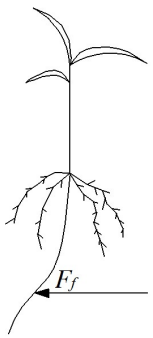

F_f is the force of the weeding spring tine.

FIGURE 2. Stress deformation diagram of a rice seedling root.

When the force F_f of the spring tine is greater than the maximum soil resistance, the weeds cannot keep still remain. Furthermore, the weeds can move in the following three ways: (a) When the action point of the force F_f exceeds the soil resistance, the weed stalk is pressed into the soil, and the weed is buried in the soil or pulled off. (b) When the action point of the force F_f is coincident with the soil resistance, the weed is pushed by the spring tine, affecting the later stage of growth and development. (c) When the action point of the force F_f is lower than the soil resistance, the weed stalk is dragged into the soil, and the weed is buried in the soil.

Analysis of the spring tine motion

The spring tine swings from side to side and moves in the forward direction with the weeding device. The motion of the spring tine can be regarded as the combined motion of uniform linear motion and reciprocating swing. Obviously, the swing plane of the spring tine and the forward direction of the device are perpendicular to each other.

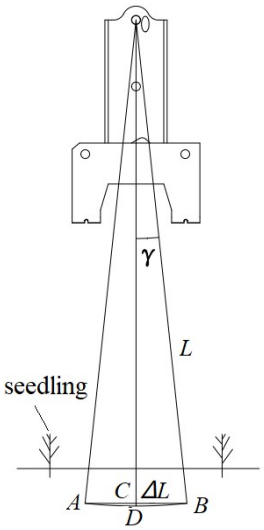

FIGURE 3. Schematic of the spring tine swing.

As shown in Figure 3, the end of the spring tine is centered at point O and swings at a certain angular velocity ω along the AB arc. Line segment CD is the vertical height change of the spring tine (in millimeters) given by

$$\begin{cases} \Delta L = L(1 - cos\gamma) \\ \gamma = \omega t \end{cases} \quad (1)$$

in which:

ΔL - the vertical height change of the spring tine, mm;

L - the length of the spring tine, mm;

γ - the swing angle of the spring tine, rad;

t - the swing time of the spring tine, s,

ω - the swing angular velocity of the spring tine, rad/s.

Since the swing range of the spring tine is not large during the weeding operations, the swing angle γ is very small. The change of vertical height ΔL, is not obvious, and it can be ignored. Therefore, in this study, arc AB of the swing trajectory at the end of the spring tine is approximately regarded as line segment AB.

From Figure 3 and [eq. (1)], the swing period T can be obtained as

$$T = \frac{4\gamma_{max}}{\omega} \quad (2)$$

in which:

T - the swing period of the spring tine, s.

By taking the forward direction as the X-axis and the swing direction of the spring tine as the Z-axis, a rectangular coordinate system is established, as shown in Figure 4.

The trajectory equation of the end point of the spring tine is:

$$\begin{cases} X = v_m t \\ Z = Lsin\gamma \end{cases} \quad (3)$$

in which:

v_m - the forward speed of the device, m/s.

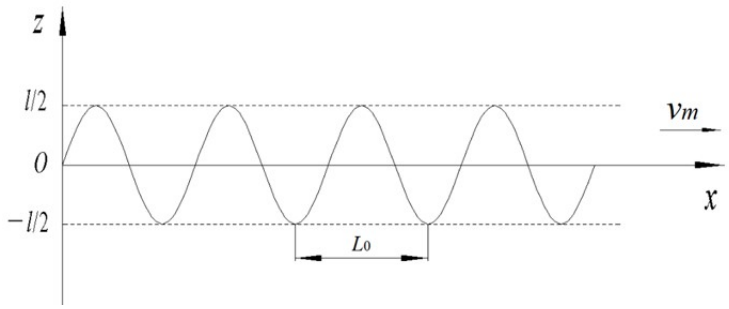

l is the swing amplitude of the spring tine, m; v_m is the forward speed of the device, m/s; L_0 is the forward distance of the device while the spring tine swings through a one cycle, m.

FIGURE 4. Trajectory of the weeding spring tine.

According to [eq. (3)], the motion track of any end point on the spring tine swinging in the horizontal plane is shown in Figure 4. L_0 is the forward distance of the device when the spring tines swing through a cycle. The smaller the value of L_0, the denser the swing of the spring tine, the smaller the probability of missing weeds in the paddy field, and the higher the weeding rate. The spring tine itself has no cutting edge, and it removes the weeds by squeezing and pushing. Therefore, the spring tine only disturbs the soil to a small extent. The movement speed of the spring tine is within a suitable range, even if the spring tine is very close to the seedling, the seedling will not be removed.

According to the above analysis, L_0 can be calculated as

$$L_0 = v_m T \tag{4}$$

According to eqs (2) and (4), the following can be obtained

$$L_0 = v_m \frac{4\gamma_{max}}{\omega} \tag{5}$$

To enhance the weeding effect and increase the weeding rate, L_0 should be appropriately decreased. It can be seen from [eq. (5)] that the forward speed of the device and the swing speed of the spring tine could affect the weeding rate of the weeding machine.

Design of the spring tine

Swing amplitude of the spring tine

According to the rice planting agronomy in China, the row spacing of rice planting is generally 300 mm, and plant spacing in the paddy is approximately 130 mm (Tian et al., 2021). The weeding range of the inter-row weeding device is about 220 mm (Saqib et al., 2015). To prevent weeds from being missed, the weeding range of the intra-row is set as 90 mm, that is, total swing amplitude of the weeding tine is 90 mm.

When the forward speed of the weeding device and swing speed of spring tine remain constant, the greater the amplitude of the weeding spring tine, the sparser the spring tine, and the lower the weeding rate. To increase the weeding rate, the swing speed of the spring tine could be appropriately increased. However, the swing speed of the spring tine increased, the absolute speed of spring tine increased, and the impact of spring tine on soil and paddy field plants got fiercer, then the rice seedling damage rate increased. To increase the weeding rate and decrease rice seedling damage rate, it is necessary to control the swing amplitude and frequency of spring tine.

In this research, three spring tines were placed on each weeding disk. In the first row, two spring tines are located at left and right; in the second row, the spring tine is located in the middle of the weeding disk. All spring tine work simultaneously. During the design, all the spring tine have the same swing amplitude, and three spring tine are arranged in two rows, and the total swing amplitude is about 90 mm. The swing amplitude l of each spring tine was 30 mm in this study.

Swing frequency of the spring tine

The spring tine is powered to swing and move in the forward direction with the weeding device. To ensure the best weeding effect, the weeding machine should be lined up before weeding. To reduce the damage of the spring tine to the seedlings, when the machine passes a plant space, the spring tine swings to the highest position from the lowest position, which is an integer multiple of the half cycle of the spring tine swing. The seedling spacing S is given by

$$\begin{cases} S = v_m t_0 \\ t_0 = \frac{n}{2} T \end{cases} \tag{6}$$

in which:

S - the seedling spacing, mm;

t_0 - the time taken for the machine to drive through a plant spacing, s,

n - any positive integer.

From the [eq. (6)], it can be get

$$\frac{S}{v_m} = \frac{n}{2} T \tag{7}$$

According to existing research (Ma et al., 2011), the forward speed of the weeding machine is generally 0.3–0.9 m/s. To suit different plant spaces, the swing frequency of the spring tine is generally 4–7 Hz.

Height of the spring tine

The spring tine is installed on the spring tine frame, and the spring tine frame is driven over the crop row with the device. To ensure smoothness of the weeding operation, the vertical height L of the spring tine should be greater than the sum of the height H of the rice seedlings and the hoeing depth h; that is,

$$L \geq H_{\max} + h_{\max} \tag{8}$$

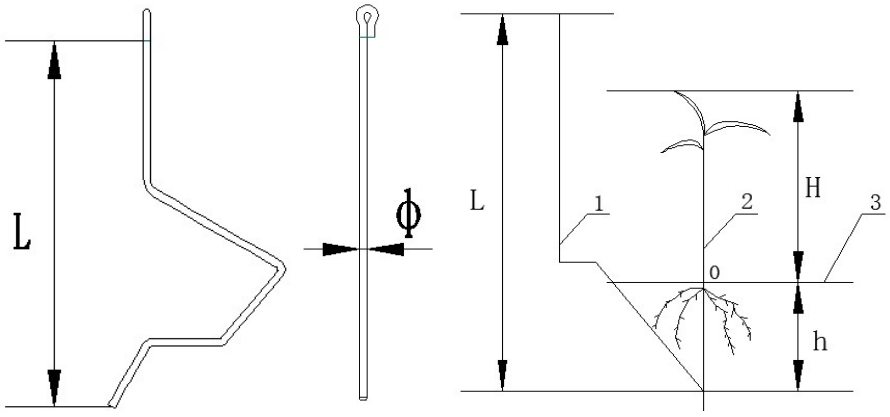

L is the height of the spring tine; and ϕ is the diameter of the spring tine; 1 is the spring tine; 2 is the seedling; 3 is the soil line; *H* is the vertical height of the spring tine; *h* is the weeding depth.

FIGURE 5. Schematic of the spring tine and hoeing depth.

When the weeding device was weeding, the spring tines directly pierce into the paddy soil to pick out or press the intra-row weeds, and the load on the spring tines was large. If the spring tines were designed in the form of vertical downward, the spring tines will be subject to large load for a long time, and it is prone to irreversible plastic deformation, which will affect the accuracy of weeding operation. In this paper, the spring tine is designed as a multi-stage bending style to increase their own elasticity. In weeding operation, the ability to resist deformation is enhanced, the service life of the spring tine is prolonged, and the weeding precision of the spring tine is increased.

Through investigation (Han et al., 2011), to ensure the weeding effect and reduce damage to the seedling root system, the hoeing depth of the spring tine-type weeding device is generally within 20–40 mm. The height of the rice seedlings was within the range of 100–150 mm at 7–10 days after transplanting, and the height of the seedlings was within the range of 200–300 mm at 15–20 days after transplanting (Wu et al., 2009; Li et al., 2015). By taking into account the structural size of the spring tine frame, the height of the spring tine *L* is 400 mm.

Diameter of the spring tine

The spring tine is the soil-contact part of the intra-row weeding device. During operation of the weeding device, the spring tine pierces the soil and swings to break and deform the soil, and the intra-row weeds in the paddy field are cut off or pulled out of the soil. Spring tines need high fatigue strength and good toughness. It is necessary to ensure that the spring tine cannot be broken and to prevent irreversible deformation of the spring tine during weeding operations. With reference to the existing research (Han et al., 2020), a *Φ* 6 mm 65 Mn spring steel wire was selected for the spring tine.

Motion analysis of the inter-row weeding device

In this paper, a wheel weeding device with rake teeth is used to remove inter-row weeds. The inter-row weeding device make circular motion around the axis under the power drive, and make uniform linear motion along the forward direction with the weeder. The motion of the inter-row weeding device can be regarded as the combined motion of uniform linear motion and uniform circular motion around the axis.

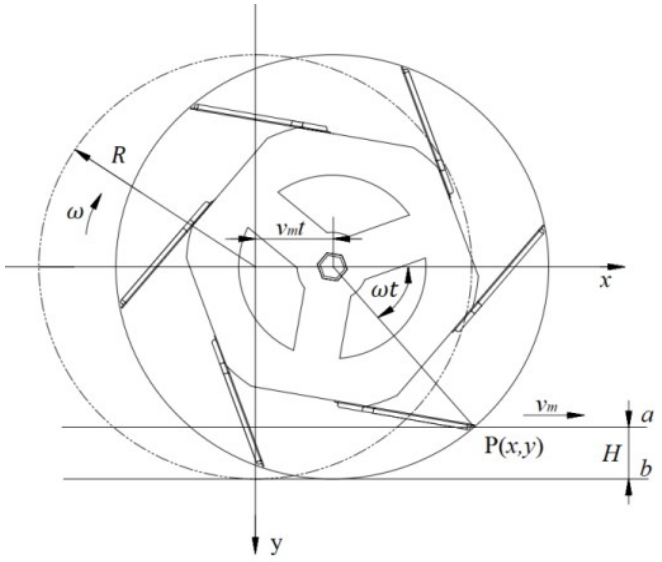

R is the radius of rotation of weeding device, mm; ω is the rotation angular velocity of weeding device, rad/s; v_m is the forward speed of the weeder, m/s; t is the working time, s; H is the weeding depth, mm; a is the soil line, b is the lowest point of weeding device motion.

FIGURE 6. Schematic diagram of the movement of the weeding wheel.

When the rotation radius of the rake teeth is r, the rotation angular velocity is ω and the forward speed of the weeder is v_m, the rectangular coordinate system as shown in Figure 6 is established. The initial rotation center of the inter-row weeding device is set as the origin of the coordinate system, the forward direction of the weeder is X-axis positive direction, and the vertical downward direction is Y-axis positive direction. Point P is the end point of rake tooth, and the initial position of point P coincides with the x-axis, then the coordinate of point P at any time is:

$$\begin{cases} x = v_m t + R\cos\omega t \\ y = R\sin\omega t \end{cases} \quad (9)$$

in which:

R - the turning radius of rake tooth, and the design value is 185 mm;

v_m - the forward speed of the weeder, m/s;

ω - the rotation angular velocity of weeding device, rad/s,

t - the working time of the weeding device, s.

The moving speed of the end point P of the rake tooth is

$$\begin{cases} v_x = \frac{dx}{dt} = v_m - R\omega\sin\omega t \\ v_y = \frac{dy}{dt} = R\omega\cos\omega t \end{cases} \quad (10)$$

The instantaneous speed of point P is

$$v = \sqrt{v_x^2 + v_y^2} = \sqrt{v_m^2 + R^2\omega^2 - 2v_m R\sin\omega t} \quad (11)$$

The circumferential speed of the end point of the weeding device is $v_P=\omega R$, so that $\lambda=v_P/v_m=\omega R/v_m$, which is called the weeding speed ratio. By substituting $\lambda=\omega R/v_m$ into [eq. (10)], thus:

$$v_x = v_m(1 - \lambda\sin\omega t) \quad (12)$$

Due to $\sin\omega t \leq 1$, when $\gamma \leq 1$, $v_x \geq 0$ is constant, the forward speed of the end point of the weeding rake tooth is always greater than zero, and the rake tooth pushes forward during operation, which can not work normally; when $\gamma > 1$, the end point of the rake teeth moves to some position, $v_x < 0$ will appear, then the rake teeth press the soil backward.

Obviously, the value of λ has a direct impact on the movement track of weeding rake teeth in the soil and the working state of weeding device.

Hoeing depth adjusting device

The hoeing depth adjusting device is an important part of the weeding machine. The hoeing depth adjusting device mentioned used here was designed on the basis of a four-bar mechanism. By means of manual adjustment, the lifting rod can be manually pulled to drive the height change of the adjusting rod, and the adjusting rod is connected to the weeding shaft. This then enables adjustment of the hoeing depth of the weeding device.

Figure 7 shows a schematic of the hoeing depth adjustment device. End A of the limit rod AB and end F of the adjusting rod FG are fixed onto the frame of the weeding device, which can rotate but cannot move. End E of the connecting rod DE is connected to the middle end E of the adjusting rod FG.

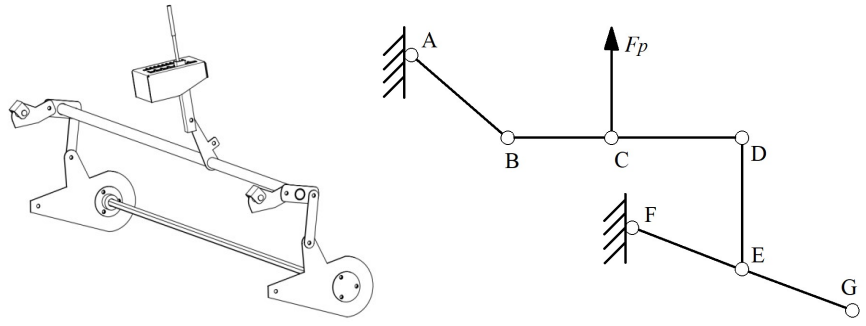

a) Structural diagram b) Structural sketch

AB is the limit rod; BD is the lifting rod; DE is the connecting rod; FG is the adjusting rod; *Fp is* pull force.

FIGURE 7. Schematic of the hoeing depth adjustment device.

The adjustment handle is installed at the midpoint position C of the lifting rod BD. When the hoeing depth of the weeding device needs to be adjusted, the block of the adjustment handle is changed, and the adjustment handle pulls the lifting rod BD to adjust its position. The lifting rod BD rotates at a certain angle around point B, and at the same time it lifts upward to a certain height. The position of the lifting rod BD changes, driving the connecting rod DE connected to it to move, and point E moves upward. End F of the adjusting rod FG is fixed; it can only be rotated but cannot be moved. Adjusting rod FG forms a lever, with end F as the fulcrum, point E as the power point, and point G as the resistance point. Manually changing the position of the adjustment handle causes the connecting rod DE to move upward. In the laborious lever FG, the power point E receives an upward pulling force, and the resistance point G moves upward. End F of adjusting rod FG is fixed to a bracket, and end G is connected to the weeding shaft. Point G moves upward, and the weeding device moves upward, thereby reducing the hoeing depth of the weeding device.

During the process of weeding, according to the growth condition of weeds in the field, the position of the adjusting handle can be changed at any time, and the

position of the weeding shaft can be changed immediately, so that the hoeing depth can be adjusted in real time.

Simulation test

Simulation tests were performed using the discrete element method to explore the changes in the mechanical behavior during the contact process between the spring tine and the soil in the paddy. The spring tine resistance moment and soil disturbance velocity were taken as the evaluation indexes of the simulation test to study the effects of different working parameters of the weeding machine on the weeding process.

When the weeding device operates in the field, the weeding spring tine produce torque due to the resistance of the soil. Due to the disturbance of weeding spring tine, the paddy soil in the original static state obtains energy, get speed and displacement. The torque of the weeding tine in the weeding operation reflects the difficulty of the weeding operation and the power consumption of the weeding device. The soil disturbance velocity reflects the destructive ability of the weeding tine to the soil, the disturbance trend of the soil and the weeding effect of the weeding operation.

With the increase of resistance moment of the spring tine, the resistance of the spring tine from the soil increased, the seedling damage rate increased, the weeding operation got difficult and operation effect got worse. The greater the soil disturbance speed, the more intense the disturbance of spring tine to paddy soil, the higher the seedling injury rate, and the worse the operation effect. In this study, the spring tine resistance moment and soil disturbance velocity were taken as indexes to analyze the change law of mechanical characteristics in the process of contact between spring tine and soil. So as to provide reference for the structural design and parameter optimization of weeding devices in paddy field.

Establishment of the simulation model

The surface soil of the paddy field during operation of the weeding device is covered with a layer of water. To simulate the soil environment of the paddy field, a contact model needs to be determined first. Particles of two different radius were established to represent water and soil. Then, the water particles were then poured onto the soil particles to allow them to penetrate downward naturally to simulate the formation of muddy water. Finally, a soil model similar to the distribution of the paddy soil is formed; that is, an upper layer is formed by the water particles, a middle layer is formed by saturated soil where water and soil particles coexist, and a lower layer is formed by the soil particles.

Adhesion between particles occurs easily because of the adhesion effect of soil. The physical structure and morphology of the soil sample are characterized by spherical granules or small clusters formed by multiple particles. In the discrete element simulation, the reduction of the particle size leads to a substantial increase in the simulation time (Bao et al., 2020). The particle size used in the discrete element simulation is generally larger than the actual size to reduce the simulation time. Therefore, to reduce the calculation time, spherical particles with a radius of 5 mm were used as soil particles, and spherical particles with a radius of 2 mm were used as water particles. A Hertz–Mindlin cohesive contact model with JKR cohesion considers the influence of van der Waals forces in the contact area and can better simulate the mechanical behavior of wet particles (Zhao et al., 2018). This model was used to study the paddy soil particle model adopted here.

In this study, the three-dimensional (3D) drawing software Unigraphics (UG) was used for structuring the model of the weeding wheel. The 3D model built was then imported into the discrete element method software EDEM in .igs format. To improve the simulation efficiency, the weeding unit of the swing-type intra-row weeding device was appropriately simplified in structure. Figure 8 shows the 3D model of the intra-row weeding monomer.

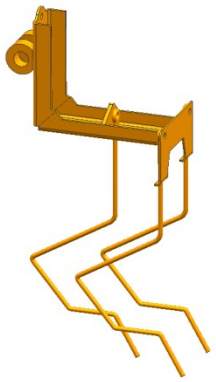

FIGURE 8. 3D model of the intra-row weeding monomer.

A virtual soil bin with length × width × height of 1000 mm × 220 mm × 100 mm was established, and the weeding monomer virtual soil bin test was performed. A total of 18,200 soil particles and 86,500 water particles were generated in the simulation test. At the beginning of the simulation, soil particles were generated in the soil bin. After the soil particles settled and stabilized, water particles were generated above them. After the water particles infiltrated the soil particles for a period of time, the weeding monomer starts to move until the simulation is completed. To ensure continuity of the simulation, the fixed time step was set to 4.15×10^{-6} s, which is 20% of the Rayleigh time step. The data-saving interval was 0.01 s. After the simulation ends, the simulation results are exported and analyzed in the EDEM post-processing tool module.

Determination of the simulation parameters

The density of water is 1000 kg/m^3, its Poisson ratio is 0.5, and its shear modulus is 0. Because a shear modulus of 0 cannot be set in EDEM, based on existing related research (Wu et al., 2017), the shear modulus of water was finally determined as 1×10^8 Pa. The density of the soil was 2000 kg/m^3, its Poisson ratio was 0.5, and its shear modulus was 1×10^8 Pa. The surface energy was determined to be 0.15 J/m^2 by a virtual experiment calibration method.

The simulation contact parameter settings used in the EDEM preprocessor are listed in Table 1.

TABLE 1. Contact parameters of the EDEM simulation.

Contact material	Coefficient of restitution	Coefficient of static friction	Coefficient of rolling friction
spring tine–soil	0.10	0.20	0.20
spring tine–water	0.05	0.05	0.01
soil–soil	0.05	0.05	0.05
soil–water	0.70	0.10	0.05
water–water	0.01	0.01	0.01

In order to reduce seedling damage, the forward speed of weeding machine should not be too high during weeding among plants. Combined with the actual operation requirements of field operation, the forward speed of weeding machine is selected as 0.3~0.9 m/s.

In the simulation test, the swing frequency of the spring tine was 5 Hz, the hoeing depth was 20 mm, and the forward speed of the machine was set to 0.30, 0.45, 0.60, 0.75, and 0.90 m/s. A single factor test was used to explore the changes in the mechanical properties of the spring tine in contact with the soil during weeding operations.

Field test

Test conditions and indices

On June 30, 2020, a field experiment of the weeding machine was conducted in Fenghuang Town, Fengtai County, Huainan City, Anhui Province. The test was performed 10 days after transplanting the seedlings, and the test area was approximately 14,000 m^2. The type of rice planted in the test fields was Nanjing 9108. The average height of rice seedlings was 260 mm, and the rice was growing well and no obvious pests and diseases were observed. No herbicides were applied to the test area. The main weeds in the test fields were barnyard grass and Leptochloa chinensis. The average height of the weeds was 110 mm, and the average root depth of the weeds was 30 mm. There were about 100 inter-row weeds in a square meter and about 25 intra-row weeds in a square meter in the test field areas. The field experiment of the weeding device in a paddy field is shown in Figure 9.

FIGURE 9. Field experiment of the weeding device in a paddy field.

The weeding rate η_1 and the rice seedling damage rate η_2 were selected as the test indices in the field test of the weeding machine. Their formulas are as follows:

$$\eta_1 = \frac{Z - Z_1}{Z} \times 100\% \quad (13)$$

$$\eta_2 = \frac{M_1}{M} \times 100\% \quad (14)$$

in which:

Z - the total number of intra-row weeds in the test area;

Z_1 - the number of intra-row weeds remaining in the test area after the weeding operation;

M_1 - the number of rice seedlings damaged by crushing, uprooting, and lodging in the test area after the weeding operation,

M - the total number of seedlings in the test area. In the test area, the weeds that were cut off, buried, and floated were all regarded as removed weeds.

The weeds in which the roots were connected to the mud surface and could continue to grow were regarded as unremoved weeds.

Test method

The weeding rate is the percentage of weeds that have been removed compared to the total number of weeds. Before weeding, the number of weeds in each test area was counted. After the weeding test was completed, the test area was closed with a string to count the number of weeds that had been removed and the number of weeds that had not been removed. Each group of data was collected three times, and the average was taken.

The rice seedling damage rate is the percentage of damaged seedlings compared to the total number of seedlings. Before weeding, the number of seedlings in each test area was counted. After the weeding test was completed, the test area was enclosed with a string to count the numbers of damaged and undamaged seedlings. The data for each group were collected three times, and the average value was taken. The overall index was estimated using the test index of the test area.

From the previous analysis, it can be seen that the forward speed of the weeding device and the hoeing depth are the main factors that affect weeding operations. The full factor test method was used to conduct field tests on the performance of the weeding machine. According to the requirements of field operation, the forward speed was selected at three levels of 0.30, 0.60, and 0.90 m/s. According to the growth characteristics of weeds and seedlings, the hoeing depth was selected at three levels: 20, 30, and 40 mm.

Second field experiment

According to the growth characteristics of paddy field weeds, a second field experiment was required. After the second weeding operation, the rice seedlings took root firmly, and the weeds germinated after that were far less robust than the seedlings and could not compete with the seedlings. Therefore, weeding operations were not required after the second weeding operation. According to the actual growth conditions of paddy field seedlings, the second weeding test was conducted on July 21, 2020, and the test method was the same as that of the first field test. Before the experiment, the weed density of rice field in the test area was counted. There were about 20 inter-row weeds in a square meter and about 6 intra-row weeds in a square meter in the test field areas.

FIGURE 10. Diagram of the second weeding test.

Multi-index comprehensive weighted score

As the optimal parameter combinations of the various factors of the weeding device under different indices could not be directly determined, it was necessary to comprehensively consider the degree of influence of each factor on the different indices to determine the optimal parameter combination.

To select the best combination of factors while considering the two indicators (weeding rate and rice seedling damage rate), a comprehensive scoring standard was established. In this study, a mapping function and multi-index comprehensive weighted evaluation method were established to evaluate the two indices.

For the weeding rate, the mapping was determined as follows:

$$f_1(x_i) = \frac{x_{max} - x_i}{x_{max} - x_{min}} (x_{min} \leq x_i \leq x_{max}) \quad (15)$$

in which:

$f_1(x_i)$ - the mapping and scoring function of the weeding rate,[0,1];

x_i - the weeding rate value of test i, %;

x_{max} - the maximum value of the weeding rate in the test results, %,

x_{min} - the minimum value of the weeding rate in the test results, %.

As the weeding rate increases, the comprehensive score increases.

For the rice seedling damage rate, the mapping was determined as follows:

$$f_2(y_i) = \frac{y_{max} - y_i}{y_{max} - y_{min}} (y_{min} \leq y_i \leq y_{max}) \quad (16)$$

in which:

$f_2(y_i)$ - the mapping and scoring function of the rice seedling damage rate, [0,1];

y_i - the rice seedling damage rate of test i, %;

y_{max} - the maximum value of the rice seedling damage rate, %;

y_{min} - the minimum value of the rice seedling damage rate in the test results, %.

As the rice seedling damage rate decreases, the comprehensive score increases.

The comprehensive weighted score Z_i for each set of tests can be expressed as follows:

$$Z_i = \omega_1 f_1(x_i) + \omega_2 f_2(y_i) \quad (17)$$

The main purpose of the weeder's work was to remove field weeds and avoid seedling damage, the optimal weight allocation of weeding rate and rice seedling damage rate is obtained as follows: ω_1=0.50, ω_2=0.50.

RESULTS AND DISCUSSION

Simulation test results

Figure 11 shows the EDEM simulation model of the weeding monomer, which simulates the soil disturbance before and after the spring tine enters the soil when the weeding device is working at a speed of 0.30 m/s.

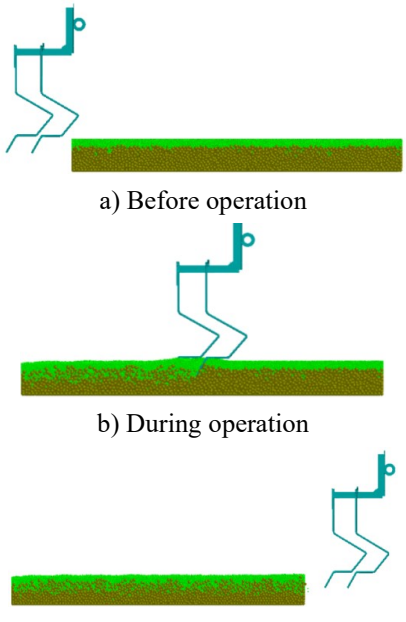

a) Before operation

b) During operation

c) After operation

FIGURE 11. EDEM simulation model of the weeding monomer.

As shown in Figure 11, when the weeding spring tine contacts the paddy field soil, the spring tine not only removes field weeds but also disturbs the paddy field soil, mixing the soil and water fully. The spring tine's disturbance of the paddy soil will increase the looseness of the paddy soil, preventing soil compaction, which is beneficial to the growth and development of crop roots and to the absorption and storage of nutrients for the paddy soil. The weeding device prevents weeds and loosens the soil and improves both rice yield and quality.

The first few seconds of the simulation were soil generation and weeding device start-up time. In this study, the test data of the constant speed operation stage of the spring tine were selected for analysis. The spring tine resistance torque curve at different forward speeds is shown in Figure 12. It can be seen from Figure 12 that the change in the forward speed has a significant effect on the contact mechanical behavior of the spring tine and the soil. When the hoeing depth and swing frequency of the spring tine remain unchanged, and the forward speed of the weeding device increases from 0.30 to 0.90 m/s, the peak resistance torque of the spring tine rises from 0.122 to 0.279 N•m., and the peak difference is 0.157 N•m, the soil resistance is obviously increased. As the forward speed increases, more soil contacts the spring tine, and the spring tine experiences more soil resistance. Therefore, the resistance torque of the spring tine increased. The weeding spring tine swings periodically, and the resistance torque of the spring tine from the soil fluctuates.

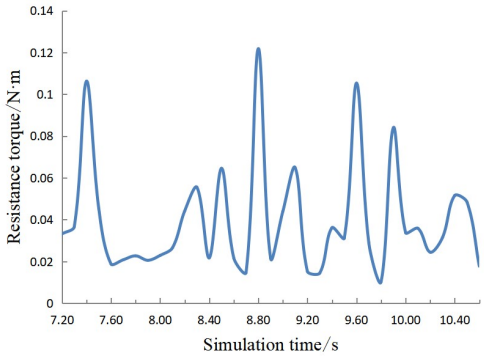

a) Forward speed is 0.30 m/s

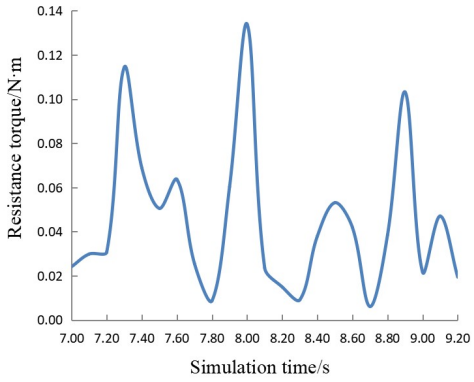

b) Forward speed is 0.45 m/s

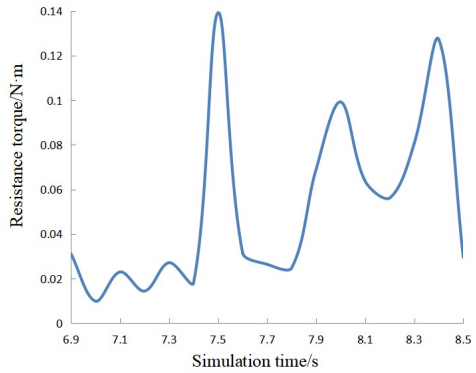

c) Forward speed is 0.60 m/s

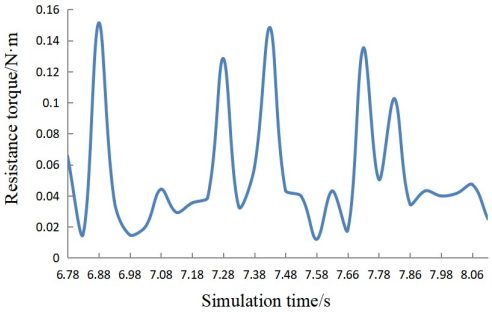

d) Forward speed is 0.75 m/s

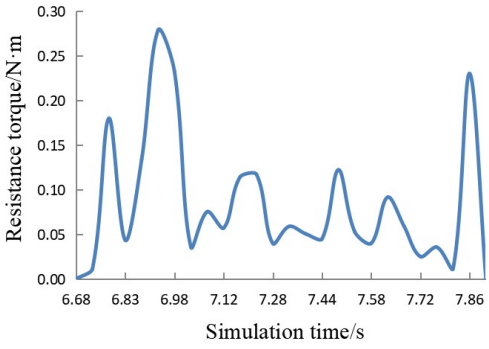

e) Forward speed is 0.90 m/s

FIGURE 12. Line charts of resistance moment of the weeding spring tine.

The soil disturbance velocity during contact between the spring tine and the paddy soil is shown in Figure 13. When the hoeing depth and swing frequency of the spring tine remain unchanged, and the forward speed of the weeding device increases from 0.30 to 0.90 m/s, the peak soil disturbance velocity rises from 0.56 to 1.23 m/s, and the peak difference is 0.67 m/s, the soil disturbance behavior is obviously aggravated. The soil particles are moved by the thrust of the spring tine, and the soil disturbance increases. Weeds in paddy fields are taken out of the soil along with the movement of the spring tine, soil disturbance is aggravated, and soil permeability increases. Therefore, the weeding effect was enhanced.

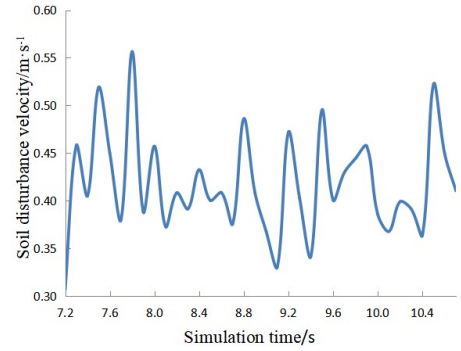

a) Forward speed is 0.30 m/s

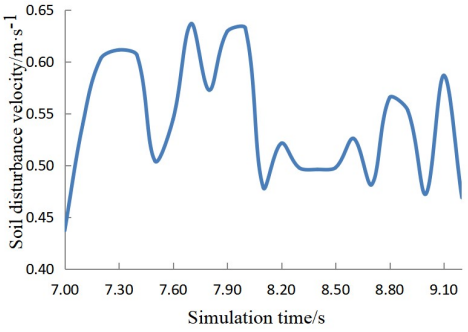

b) Forward speed is 0.45 m/s

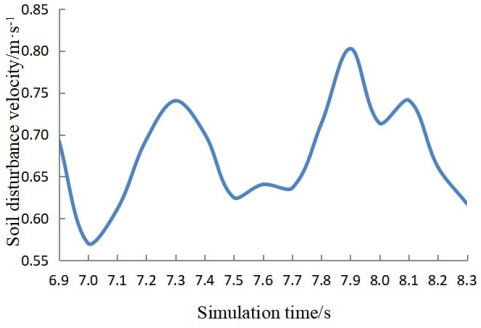

c) Forward speed is 0.60 m/s

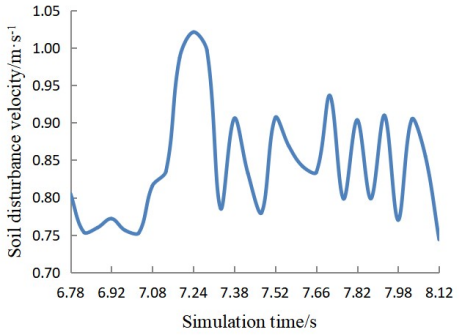

d) Forward speed is 0.75 m/s

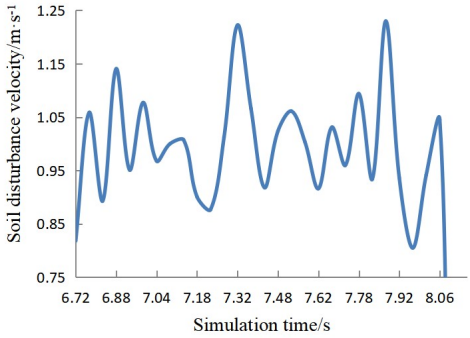

e) Forward speed is 0.90 m/s

FIGURE 13. Line charts of the soil disturbance velocity.

Field test results

After the field test was performed, the numbers of weeds and damaged seedlings were counted, and the measured test data were averaged and recorded.

TABLE 2. Field experiment data for the weeding machine.

Test No.		Forward speed A (m/s)	Hoeing depth B (mm)	Weeding rate η_1 (%)	Damage rate η_2 (%)
1		0.30	20	81.7	2.3
2		0.30	30	83.5	2.8
3		0.30	40	85.0	3.4
4		0.60	20	80.8	3.9
5		0.60	30	82.2	4.6
6		0.60	40	83.4	5.3
7		0.90	20	79.6	3.6
8		0.90	30	81.3	4.2
9		0.90	40	82.0	4.7
η_1	K_1	250.2	242.1		
	K_2	246.4	247.0		
	K_3	242.9	250.4		
	R	7.3	8.3		
η_2	K_1	8.5	9.8		
	K_2	13.8	11.6		
	K_3	12.5	13.4		
	R	5.3	3.6		

Note: In the table, the values in K_1~K_3 and R correspond to the sum and range of weeding rate and damage rate respectively.

From the results of the range analysis in Table 2, it can be seen that the weeding rate is more strongly affected by the hoeing depth than by the forward speed. As the hoeing depth increases, the area of action between the spring tine and the paddy soil increases, and the ability to act on weeds increases, so the weeding rate continues to rise, reaching its maximum at a depth of 40 mm. When the forward speed of the device increases, the absolute speed at the end of the spring tine increased, and the force of the spring tine on the weeds increases, so that the weeding rate increases accordingly. However, as the forward speed increases, the trajectory of the spring tine in the weeding area becomes sparse, the actual weeding area decreases, and the weeding rate decreases accordingly. Therefore, as the forward speed of the machine increases, the weeding rate decreases to a certain extent.

The rice seedling damage rate is more affected by the forward speed than by the hoeing depth. As the forward speed of the machine increases, the damage rate increases and then decreases. As the forward speed of the machine increases, the force of the weeding spring tine on the seedlings also increases, resulting in damage to the seedlings. When the forward speed of the machine increases, the trajectory of the spring tine becomes sparse, the probability of contact with the seedlings is reduced, and the rate of damage to the seedlings is therefore reduced. The depth of weeding affects the rate of damage to seedlings. When the hoeing depth increased, the effect of the spring tine and the roots of the seedlings increases because of the deeper tillage, and the rate of damage to the seedlings increases.

For a comprehensive consideration of the weeding rate and rice seedling damage rate for different factors, we referred to the weeder's technical specifications to evaluate the quality of the seedling weeder (DB23/T930-2005). The specifications give a weeding rate of ≥80% and a rice seedling damage rate of ≤5%. It can be concluded that the weeding device meets the technical specifications and meets the weeding requirements. The results of the field test are basically consistent with the simulation results, which verify the feasibility of the simulation test.

Replace the weeding rate and rice seedling damage rate in Table 2 into formula (13) to get the comprehensive weighted score, as shown in table 3.

TABLE 3. Comprehensive weighted grading results of field test of the weeding machine.

Test No.	Forward speed A(m/s)	Hoeing depth B(mm)	Weeding rate η_1(%)	Damage rate η_2(%)	Z
1	0.30	20	81.7	2.3	0.694
2	0.30	30	83.5	2.8	0.4111
3	0.30	40	85.0	3.4	0.8166
4	0.60	20	80.8	3.9	0.3444
5	0.60	30	82.2	4.6	0.3574
6	0.60	40	83.4	5.3	0.3519
7	0.90	20	79.6	3.6	0.3500
8	0.90	30	81.3	4.2	0.3468
9	0.90	40	82.0	4.7	0.3222

According to the data in table 3, when the forward speed is 0.30 m/s and the hoeing depth is 40 mm, the weeding device can achieve better performance.

Results of the second weeding experiment

After the second weeding operation of the weeding device, the number of weeds and injured seedlings in each test area were counted respectively, and the average value of the measured test data was recorded as shown in Table 4.

TABLE 4. The second field experiment data of the weeding machine.

Test No.	Forward speed A(m/s)	Hoeing depth B(mm)	Weeding rate η_1(%)	Damage rate η_2(%)
1	0.30	20	83.0	1.7
2	0.30	30	84.8	2.3
3	0.30	40	86.3	2.9
4	0.60	20	82.5	3.4
5	0.60	30	83.5	4.1
6	0.60	40	84.7	4.3
7	0.90	20	81.9	2.9
8	0.90	30	82.6	3.7
9	0.90	40	83.3	4.2

After the first weeding operation, the number of weeds in the field decreased significantly, and the weeding effect met the expected requirements. Because the weed density of the second weeding is small, and the rice seedlings are relatively strong, the phenomenon of rice seedling damage is not obvious, so the weeding rate is higher than that of the first weeding, and the rice seedling damage rate is lower than that of the first weeding. The results showed that the rice seedlings rooted thoroughly in the paddy field and were stronger than weeds in the second weeding operation. After two weeding operations, the rice seedlings were strong enough, and the subsequent germination weeds were difficult to compete with the seedlings.

Discussion

The mechanical behavior of the spring tine changes constantly when it contacts the paddy soil. The forward speed of the device has a significant effect on the mechanical behavior of the spring tine when it contacts the soil. When the soil properties remain unchanged, as the forward speed of the machine increases, the resistance torque of the spring tine increases, and the soil disturbance velocity increases.

The higher the forward speed, the greater the resistance torque of the spring tine, the greater the force of the spring tine on field plants during machine operation, the greater the abrasion of the spring tine, and the greater the energy consumption of the machine during operation. The greater the forward speed, the greater the soil disturbance velocity. When the spring tine is operating in the field, disturbance to the paddy soil is aggravated, and the weeding effect of the weeding device is improved. When other conditions remain unchanged, the increase in the forward speed of the device makes the spring tine contact more soil at the same time, and the spring tine acts on more soil.

The friction between spring tine and soil is carried out through the contact area, so the shape of each surface plays a critical role in the friction. The contact area between spring tine and soil is a mixture of water film, colloid, pollutant and soil particle. The relative sliding of spring tine and soil is essentially the rheology of the material in the contact area. Because the above composition is obviously different from the typical Newtonian fluid, such as water, gas and so on. At this point, the soil can be considered as a non-Newtonian fluid with dilatancy. When the forward speed of weeding device increases, the soil viscosity increases with the increase of spring tine speed. The friction between the soil and the spring tine increases, and the resistance moment of the spring tine increases macroscopically.

During the operation of the weeding device, the weeding spring tine contact with the paddy soil, and the spring tine stir the paddy soil to pull out or press the weeds into the soil. The more disturbed the soil is, the easier weeds are removed and the higher the weeding rate is. The greater the soil resistance moment is, the greater the power of the machine is, and the greater the energy consumption of the weeding device is.

Comprehensively considered, the weeding device needs to adapt to the change of mechanical behavior of the contact between the spring tine and soil, select appropriate working parameters to reduce the soil disturbance velocity and spring tine resistance moment. So as to improve the weeding rate and reduce the rice seedling damage rate.

CONCLUSIONS

The weeding machine designed in this study is suitable for the prevention and control of paddy field weeds in rice production. It can remove inter-row and intra-row weeds in paddy fields. The principle of avoiding seedlings while weeding is ingenious, and the production cost is low. The results of this study are as follows;

(1) A weeding machine for paddy fields was designed. The working principle of the weeding machine was analyzed, the motion track of the spring tine was analyzed, and the structural parameters of the weeding device were determined.

(2) The interaction between the spring tine and the soil in the paddy was simulated using the discrete element method. The change in the orderliness of the mechanical behavior during the interaction between the spring tine and the soil in the paddy was recorded. The influence of the forward speed of the weeding machine on the resistance torque of the spring tine and on the soil disturbance velocity was analyzed.

(3) The forward speed and the hoeing depth were taken as experimental factors, and the weeding rate and rice seedling damage rate were selected as test indices. Field experiments were performed to study the effects of each factor on weeding operations. The test results were evaluated by multi index comprehensive weighting. The results showed that when the forward speed was 0.30 m/s and the hoeing depth was 40 mm, the weeding rate was 85.0% and the rice seedling damage rate was 3.4%. The weeding effect of the machine was the best.

(4) All straws were returned to the field after the rice was harvested, and the weeding device was entangled by weeds and straws during the operation of the weeding device. The spring tine needs to penetrate the soil to work, and the work resistance is relatively large. Research on the mechanism of drag reduction and entanglement prevention of weeding devices will be the focus of our next work.

(5) When the weeding device operates in the field, without affecting the operation efficiency, the forward speed of the weeding machine should be appropriately reduced to make the weeding spring tine contact more soil, so as to obtain higher weeding rate and lower seedling damage rate.

ACKNOWLEDGMENTS

The project was supported by the National Natural Science Foundation of China (51475002 and 52105239), Major Science and Technology Projects of Anhui Province (17030701046), and the Natural Science Foundation of Anhui Province (2008085QE270 and 1808085QE171).

REFERENCES

Agriculture-Field Crops (2020) New Findings from University of Catania in the Area of Field Crops Published (Integrated Weed Management in Herbaceous Field Crops). Agriculture Week.

Bao Yudong, Yang Jie, Zhao Yanling, Liu Xianli, Guo Yanling, Li Zhipeng, Xiang Jingzhong (2020) Design of the walking driving system for a blueberry harvester based on contact mechanical behavior of wheel-soil. Transactions of the Chinese Society of Agricultural Engineering 36(7): 43–52. DOI: https://doi.org/10.11975/j.issn.1002-6819.2020.07.005

Åstrand B, Baerveldt AJ (2002) An agricultural mobile robot with vision-based perception for mechanical weed control. Autonomous Robots 13(1): 21–35. DOI: https://doi.org/10.1023/A:1015674004201

Chen Z, Li N, Sun Z, Li T, Zhang C, Li W (2015a) Optimization and experiment of intra-row brush weeding manipulator based on planetary gear train. Transactions of the Chinese Society for Agricultural Machinery 46(09): 94–99. DOI: https://doi.org/10.6041/j.issn.1000-1298.2015.09.013

Chen Z, Zhang C, Li N, Sun Z, Li W, Zhang B (2015b) Study review and analysis of high performance intra-row weeding robot. Transactions of the Chinese Society of Agricultural Engineering 31(5): 1–8. DOI: https://doi.org/10.3969/j.issn.1002-6819.2015.05.001

Pannacci E, Farneselli M, Guiducci M, Tei F (2020) Mechanical weed control in onion seed production. Crop Protection 135(105221). DOI: https://doi.org/10.1016/j.cropro.2020.105221

Han B, Guo C, Gao Y, Liu Q, Sun S, Dong X (2020) Design and experiment of soybean weeding monomer mechanism and key components. Transactions of the Chinese Society for Agricultural Machinery 51(6):112-121. DOI: https://doi.org/10.6041/j.issn.1000-1298.2020.06.012

Han B, Shen J, Li Y (2011) Design and experiment of 3ZCF-7700 multi-functional weeding-cultivating machine. Transactions of the Chinese Society of Agricultural Engineering 27(1): 124–129. DOI: https://doi.org/10.3969/j.issn.1002-6819.2011.01.019

Hu L, Luo X, Yan Y, Chen X, Zen S, Zhang L (2012) Development and experiment of intra-row mechanical weeding device based on trochoid motion of claw tooth. Transactions of the Chinese Society of Agricultural Engineering 28(14): 10–16. DOI: https://doi.org/10.3969/j.issn.1002-6819.2012.14.002

Hu L, Luo X, Zhang Z, Chen X, Lin C (2013) Side-shift offset identification and control of crop row tracking for intra-row mechanical weeding. Transactions of the Chinese Society of Agricultural Engineering 29(14): 8–14. DOI: https://doi.org/10.3969/j.issn.1002-6819.2013.14.002

Jia H, Li S, Wang G, Liu H (2018) Design and experiment of seedling avoidable weeding control device for intertillage maize (Zea Mays L.). Transactions of the Chinese Society of Agricultural Engineering 34(7): 15–22. DOI: https://doi.org/10.11975/j.issn.1002-6819.2018.07.002

Li N, Chen Z, Zhu C, Zhang C, Sun Z, Li W (2016) System design and experiment of electric driven weeding robot. Transactions of the Chinese Society for Agricultural Machinery 47(05): 15–20, 69. DOI: https://doi.org/10.6041/j.issn.1000-1298.2016.05.003

Li Z, Ma X, Qi L, Tan S, Chen X, Tan Y, Liang Z, Sun G, Huang Y (2015) Comparison and evaluation of different rice mechanized transplanting methods in double cropping area of South China. Transactions of the Chinese Society of Agricultural Engineering 31(3): 40–47. DOI: https://doi.org/10.3969/j.issn.1002-6819.2015.03.006

Boone L, Roldán-Ruiz I, Van Linden V, Muylle H, Dewulf J (2019) Environmental sustainability of conventional and organic farming: Accounting for ecosystem services in life cycle assessment. Science of the Total Environment 695(11834). DOI: https://doi.org/10.1016/j.scitotenv.2019.133841

Ma X, Qi L, Liang B, Tan Z, Zuo Y (2011) Present status and prospects of mechanical weeding equipment and technology in paddy field. Transactions of the Chinese Society of Agricultural Engineering 27(6): 162–168. DOI: https://doi.org/10.3969/j.issn.1002-6819.2011.06.030

Pérez-Ruíz M, Slaughter DC, Fathallah FA, CJ Gliever, BJ Miller (2014) Co-robotic intra-row weed control system. Biosystems Engineering 126: 45 – 55. DOI: https://doi.org/10.1016/j.biosystemseng.2014.07.009

Persson M, Åstrand B (2008) Classification of crops and weeds extracted by active shape models 100(4): 484 – 497. DOI: https://doi.org/10.1016/j.biosystemseng.2008.05.003

Home M (2003) An investigation into the design of cultivation systems for inter-and intra-row weed control. PhD Thesis, Cranfield University, Silsoe National Soil Resources Institute.

Tillett ND, Hague T, Grundy AC, Dedousis AP (2007) Mechanical within-row weed control for transplanted crops using computer vision. Biosystems Engineering 99(2): 171–178. DOI: https://doi.org/10.1016/j.biosystemseng.2007.09.026

Niu C, Wang J (2010) Analysis on working mechanism of paddy weeding device. Transactions of the Chinese Society of Agricultural Engineering 26(1): 51–55. DOI: https://doi.org/10.3969/j.issn.1002-6819.2010.z1.012

Alba OS, Syrovy LD, Duddu HSN, Shirtliffe SJ (2020) Increased seeding rate and multiple methods of mechanical weed control reduce weed biomass in a poorly competitive organic crop. Field Crops Research 245(107648). DOI: https://doi.org/10.1016/j.fcr.2019.107648

Qi L, Liang Z, Jiang Y, Ma X, Wu T, Lu Y, Zhao L (2016) Design and field test of lightweight paddy weeder. Journal of Jilin University (Engineering and Technology Edition) 46(03): 1004–1012. DOI: https://doi.org/10.13229/j.cnki.jdxbgxb20160348

Qi L, Liang Z, Ma X, Tan Y, Jiang L (2015) Validation and analysis of fluid–structure interaction between rotary harrow weeding roll and paddy soil. Transactions of the Chinese Society of Agricultural Engineering 31(05): 29–37. DOI: https://doi.org/10.3969/j.issn.1002-6819.2015.05.005

Qi L, Zhao L, Ma X, Cui H, Zheng W, Lu Y (2017) Design and test of 3GY-1920 wide-swath type weeding-cultivating machine for paddy. Transactions of the Chinese Society of Agricultural Engineering 33(08): 47–55. DOI: https://doi.org/10.11975/j.issn.1002-6819.2017.08.006

Saqib M, Ehsanullah AN, Latif M, Ijaz M, Ehsan F, Ghaffar A (2015) Development and appraisal of mechanical weed management strategies in direct seeded aerobic rice (Oryza Sativa L.). Pakistan Journal of Agricultural Sciences 52(3): 587–593.

Tao G, Wang J, Zhou W, Niu C, Zhao J (2015) Herbicidal mechanism and key components design for paddy weeding device. Transactions of the Chinese Society for Agricultural Machinery 46(11): 57-63. DOI: https://doi.org/10.6041/j.issn.1000-1298.2015.11.009

Tian Z, Lu J, Yuan G, Shen G (2020) Effects and eco-economic thresholds of Leptochloa chinensis and Cyperus difformis on the yield of direct-seeding rice. Chinese Journal of Eco-agriculture 28(03): 328–336. DOI: https://doi.org/10.13930/j.cnki.cjea.190755

Tian L, Cao C, Qin K, Fang L, Ge J (2021) Design and test of post-seat weeding machine for paddy. International Journal of Agricultural and Biological Engineering 14(3):112-122. DOI: 10.25165/j.ijabe.20211403.5936

Wang J, Gao G, Yan D, Wang J, Weng W, Cheng B (2018) Design and experiment of electric control double row deep fertilizing weeder in paddy field. Transactions of the Chinese Society for Agricultural Machinery 49(07): 46 - 57. DOI: https://doi.org/10.6041/j.issn.1000-1298.2018.07.006

Wang J, Wang J, Yan D, Tang H, Zhou W (2017) Design and experiment of 3SCJ-2 type row weeding machine for paddy field. Transactions of the Chinese Society for Agricultural Machinery 48(06): 71–78, 202. DOI: https://doi.org/10.6041/j.issn.1000-1298.2017.06.009

Wu C, Zhang M, Jin C, Tu A, Lu Y, Xiao T (2009) Design and experiment of 2BYS-6 type paddy weeding-cultivating machine. Transactions of the Chinese Society for Agricultural Machinery 40(07): 51–54.

Wu L, Qi S, Song Y, Xin M, Liu C, Kong A, Jiao Z, Liu F, Ren W (2017) A DEM analysis on drag reduction characteristics of paddy field machinery surface with bionic microarchitectures. Journal of Shenyang Agricultural University 48(01): 55–62. DOI: https://doi.org/10.3969/j.issn.1000-1700.2017.01.008

Xu G, Wang H, Zhai Z, Sun M, Li Y (2015) Effect of water and nitrogen coupling on root morphology and physiology, yield and nutrition utilization for rice. Transactions of the Chinese Society of Agricultural Engineering 31(10): 132–141. DOI: https://doi.org/10.11975/j.issn.1002-6819.2015.10.018

Yang C, Liu L, Chun NT, Qin H, Zhao Q, Chen D, Xu S, Huang M, Jiang L (2016) Effects of soil moisture on root growth of no-tillage rice. Journal of Huazhong Agricultural University 35(01): 8 - 16. DOI: https://doi.org/10.13300/j.cnki.hnlkxb.2016.01.002

Zhang H, Gong J (2014) Research status and development discussion on high-yielding agronomy of mechanized planting rice in China. Scientia Agricultura Sinica 47(07): 1273–1289. DOI: https://doi.org/10.3864/j.issn.0857-1752.2014.07.004

Zhang X, Chen Y (2017). Soil disturbance and cutting forces of four different sweeps for mechanical weeding. Soil & Tillage Research (168): 167–175. DOI: https://doi.org/10.1016/j.still.2017.01.002

Zhang Z, Li Y, Zhang B, Yang X (2014) Influence of weeds in Echinochloa on growth and yield of rice. Chinese Journal of Applied Ecology 25(11):3177–3184. DOI: https://doi.org/10.13287/j.1001-9332.20140829.005

Zhao J, Ding Q, Zhang W, Yu S (2018) Coupling analysis of transplanter wheel and paddy soil in steering process. Chinese Journal of Soil Science 49(6): 1319–1325. DOI: https://doi.org/10.19336/j.cnki.trtb.2018.06.08

Zheng J, Wang W, Liu G, Ding Y, Cao X ,Chen D, Engel BA (2020) Towards quantification of the national water footprint in rice production of China: A first assessment from the perspectives of single-double rice. Science of the Total Environment 793. DOI: https://doi.org/10.1016/j.scitotenv.2020.140032

Zhou F, Wang W, Li X, Tang Z (2018). Design and experiment of cam rocker swing intra-row weeding device for maize. Transactions of the Chinese Society for Agricultural Machinery 49(01): 77–85. DOI: https://doi.org/10.6041/j.issn.1000-1298.2018.01.009

Zhou Y, Cheng L, Wang W, Li Z, Zeng Y, Tan X, Hu S, Shi Q, Pan X, Zeng Y (2020) Effects of different direct seeding methods and weed control timing on weed occurrence and grain yield of early indica rice. Acta Prataculturae Sinica 29(5): 132 - 140. DOI: https://doi.org/10.11686/cyxb2019421

Zhou Y, Wang W, Chen L, Zeng Y, Tan X, Hu S, Shi Q, Pan X, Zeng Y (2019) Progress on weed occurrence and control in direct seeded rice fields. Crops (04): 1–9. DOI: https://doi.org/10.16035/j.issn.1001-7283.2019.04.001

Zhu D, Zhang Y, Chen H, Xiang J, Zhang Y (2015) Innovation and practice of high-yield rice cultivation technology in China. Scientia Agricultura Sinica 48(17): 3404–3414. DOI: https://doi.org/10.3864/j.issn.0578-1752.2015.17.008